Article

A hydrogel-microsphere drug delivery system that supports once-monthly administration of a GLP-1 receptor agonist

Eric L Schneider, Brian R Hearn, Samuel J. Pfaff, Ralph Reid, David G. Parkes, Niels Vrang, Gary W. Ashley, and Daniel V. Santi

ACS Chem. Biol., **Just Accepted Manuscript** • Publication Date (Web): 12 Jun 2017

A hydrogel-microsphere drug delivery system that supports once-monthly administration of a GLP-1 receptor agonist

Eric L. Schneider[1], Brian R. Hearn[1], Samuel J. Pfaff[1], Ralph Reid[1], David G. Parkes[2], Niels Vrang[3], Gary W. Ashley[1] and Daniel V. Santi[1,4] *

[1] ProLynx, 455 Mission Bay Blvd. South, Suite 145, San Francisco, CA 94158
[2] DGP Scientific Inc, 156 Melanie Way, Del Mar, CA 92014
[3] Gubra ApS, Horsholm Kongevej 11B, 2970 Horsholm, Denmark
[4] Department of Pharmaceutical Chemistry, University of California, San Francisco, 600 16th Street, San Francisco, California 94158, United States

* Corresponding author: Daniel V. Santi, ProLynx, 455 Mission Bay Blvd. South, Suite 145, San Francisco, CA 94158; Daniel.V.Santi@prolynxllc.com. Phone 415 552 5306

Abstract

We have developed a chemically-controlled very long-acting delivery system to support once-monthly administration of a peptidic GLP-1R agonist. Initially, the prototypical GLP-1R agonist exenatide was covalently attached to hydrogel microspheres by a self-cleaving β-eliminative linker; after subcutaneous injection in rats the peptide was slowly released into the systemic circulation. However, the short serum exenatide half-life suggested its degradation in the subcutaneous depot. We found that exenatide undergoes deamidation at Asn^{28} with an *in vitro* and *in vivo* half-life of approximately two weeks. The [Gln^{28}]exenatide variant and exenatide showed indistinguishable GLP-1R agonist activities as well as pharmacokinetic and pharmacodynamic effects in rodents; however, unlike exenatide, [Gln^{28}]exenatide is stable for long periods. Two different hydrogel-[Gln^{28}]exenatide conjugates were prepared using β-eliminative linkers with different cleavage rates. After subcutaneous injection in rodents, the serum half-lives for the released [Gln^{28}]exenatide from the two conjugates were about two weeks and one month. Two monthly injections of the latter in the Zucker diabetic fatty rat showed pharmacodynamic effects indistinguishable from two-months of continuously infused exenatide. Pharmacokinetic simulations indicate that the delivery system should serve well as a once-monthly GLP-1R agonist for treatment of Type 2 diabetes in humans.

Introduction

Peptidic GLP-1 receptor agonists (GLP-1RA) have emerged as an important standard-of-care drug class for the treatment of Type 2 diabetes (T2D)[1]. These agonists stimulate glucose-mediated insulin secretion, suppress inappropriately elevated glucagon secretion and slow gastric emptying. Additionally, GLP-1RAs show potentially beneficial non-glycemic effects [2, 3]. First, because they increase satiety and reduce food intake, they may have utility as anti-obesity agents [4-6]. Second, as demonstrated for liraglutide [7] and semaglutide [8], the drug class may reduce the risks for adverse cardiovascular events in patients with T2D [9, 10]. Third, GLP-1RAs may prevent or ameliorate certain cognitive disorders [3] and, finally, as recently shown for liraglutide, may be efficacious in treatment of non-alcoholic steatohepatitis [11].

Exendin-4, a 39-amino acid peptide isolated from salivary secretions of the Gila monster, is the prototypical GLP-1RA [12]. Synthetic exenatide is marketed for treatment of patients with T2D as Byetta® that – with an elimination half-life ($t_{1/2,\beta}$) of only ~2.5 hr – requires twice daily subcutaneous (SC) injections. There is both demand for and benefit in longer-acting GLP-1RA delivery systems, and a number of once-daily and once-weekly (QW) administered agonists have been developed for treatment of T2D [1, 13]. These longer-acting agonists show a greater reduction in fasting glucose and HbA1c than exenatide, a decreased incidence of nausea and vomiting, and improved patient convenience and compliance [1]. Nevertheless, poor medication adherence and persistence remain as major contributing factors leading to failure of glycemic control in patients with T2D [14]. As observed with other chronic diseases, patient compliance and persistence in taking medications for T2D should improve as the dosing interval increases [15-17]. Thus, the development of even longer acting GLP-1RAs with increased convenience, compliance, persistence and, hopefully, therapeutic efficacy is a major and timely challenge.

Although no once-monthly (QM) GLP-1RAs have yet emerged, several attempts have been made to adapt QW agonists to longer-acting therapeutics. For example, the QW PLGA-encapsulated exenatide, Bydureon, has been reformulated as a suspension in medium-chain triglycerides for QM administration [18]. Although the QM suspension increased the proportion of patients that achieved target HbA1c levels, the impracticably high viscosity of the formulation and its necessity for caregiver administration [19] will not address problems of compliance and persistence. Also, QW GLP-1 peptide agonist fusions of Fc [20], albumin [21] or XTEN [22, 23] with half-lives of 5 to 6 days have been administered QM at doses sufficient to maintain therapeutic levels over multiple half-lives; here, the consequential high C_{max} and peak-to-trough (C_{max}/C_{min}) ratios >10 likely exceed tolerability limits. An ideal QM GLP-1RA would have a half-life of about one month, a C_{max}/C_{min} within known tolerable limits, and be patient-administrable as a low-volume, painless SC injection using an auto-syringe with a small bore needle. An implantable osmotic pump that efficiently delivers exenatide over six months is in clinical trials [24], but patient-acceptance of a surgically implanted device remains uncertain.

We have developed a general approach for half-life extension of therapeutics in which a drug is covalently tethered to a long-lived carrier by a linker that slowly cleaves to release the native drug [25, 26]. Here, the linker is attached to a drug *via* a carbamate group (**1; Scheme 1**); the β-carbon has an acidic carbon–hydrogen bond (C–H) and also contains an electron-withdrawing "modulator" (Mod) that controls the pK_a of that C–H bond. Upon proton removal to give **2**, a rapid β-elimination occurs, cleaving the linker-carbamate bond and releasing the free drug. The rate of drug release is proportional to the acidity of the proton, which is controlled by the electron withdrawing ability of the pK_a modulator. These linkers are not affected by enzymes and are stable for years when stored at low pH and temperatures [25].

Scheme 1

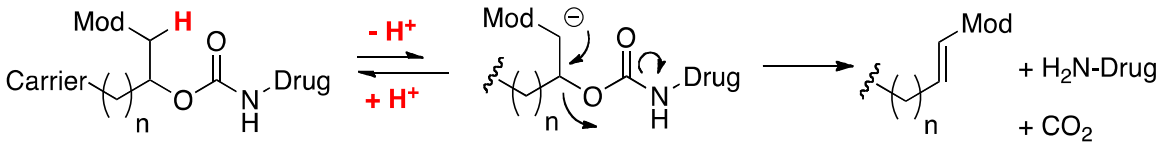

1 **2** **3**

One carrier we use is a large-pore Tetra-PEG hydrogel polymer that presents little barrier to diffusion of released drugs [26, 27]. These hydrogels are fabricated as uniform single-molecule ~40 μm microspheres by a microfluidic device [28] and can be easily injected SC through a small-bore needle. We also incorporate slower cleaving β-eliminative linkers in each of the crosslinks of these polymers, so gel degradation can be adjusted to occur after drug release. Using linkers with different pre-programed cleavage rates to connect microspheres to drugs, the elimination half-lives of peptidic drugs have been increased from under one hour to weeks or months [28, 29].

We previously reported a releasable Tetra-PEG hydrogel-exenatide conjugate that after SC administration provides systemic exenatide with a $t_{1/2,\beta}$ of ~7 days in the rat, and should support QW administration of exenatide in the human [28]. This conjugate appears comparable to current QW GLP-1 agonists, but the several weekly agonists already on the market reduce impetus for its clinical development.

In the present work, we describe experiments that led to the development of the first GLP-1 agonist that could be effectively administered by once-monthly SC administration in humans.

Results

Pharmacokinetics of a hydrogel-exenatide depot. **Scheme 2** shows the three consecutive reactions that occur after SC injection of non-circulating cleavable-conjugates. The conjugate releases drug by rate constant k_1 in the SC compartment ($Drug_{SC}$), which then enters the central compartment ($Drug_{CC}$) with k_a from which it is eliminated with rate constant k_2. If, as in the present case, $k_2 > k_a > k_1$, the concentration of $Drug_{CC}$ at any time is described by eq. 1, where CL is the drug clearance and F is the bioavailability [28].

Scheme 2

$$\text{Gel-Drug}_{SC} \xrightarrow{k_1} \text{Drug}_{SC} \xrightarrow{k_a} \text{Drug}_{CC} \xrightarrow[\text{elimination}]{k_2}$$

$$[\text{Drug}]_{CC,t} = \text{Dose} \cdot \frac{F}{CL} \cdot k_1 \cdot (e^{-k_1 t} - e^{-k_a t}) \qquad [1]$$

We recently reported a releasable hydrogel-exenatide conjugate with a $MeSO_2$- modulator in the β-eliminative linker that showed a $t_{1/2,\beta}$ for released exenatide of one week in the rat [28]. We sought to increase the $t_{1/2,\beta}$ and studied a hydrogel having a linker with a -CN modulator designed to give ~4-fold slower drug release [25].

We prepared N^{α}-[(7-azido-1-cyano-2-heptyloxy)carbonyl]exenatide (N_3L[CN]-exenatide) by SPPS and attached it by strain-promoted alkyne-azide cycloaddition (SPAAC) to monofluorocyclooctyne (MFCO)-derivatized Tetra-PEG hydrogels [27, 28]. Under accelerated release conditions, the conjugate showed an extrapolated *in vitro* release $t_{1/2}$ of 2,020 hrs at pH 7.4, 37 °C.

Since *in vitro* release of exenatide from a β-eliminative linker is ~2-fold slower than *in vivo* release [28], we anticipated an *in vivo* $t_{1/2,\beta}$ of ~1,000 hr for the released exenatide. However, a pharmacokinetic study of the SC hydrogel-exenatide conjugate in the rat showed a $t_{1/2,\beta}$ of only 240 hr (**Fig. 1**). Using eq. 1, the expected $t_{1/2,\beta}$ of 1,000 hr and pharmacokinetic parameters of exenatide in the rat [30], we simulated the expected C vs t plot in the rat (**Fig. 1**). The observed $t_{1/2,\beta}$ was about 4-fold lower and the AUC_{inf} was only ~10% of that expected.

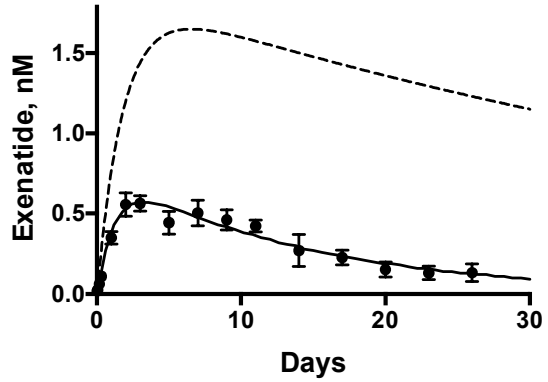

Figure 1. Pharmacokinetics of a hydrogel-L[CN]-exenatide conjugate containing 0.42 μmol exenatide in the rat. The solid line (-③-) shows serum exenatide in the rat from a SC hydrogel-exenatide showing an observed $t_{1/2,\beta}$ of 240 hr and 10% of the expected AUC_{inf}; error bars show ±SEM. The dashed line (---) shows the expected C vs t for released exenatide assuming a $t_{1/2,\beta}$ of 1,000 hr.

We considered the possibility that the low $t_{1/2,\beta}$ and AUC of the released exenatide was due to degradation of the peptide in the SC depot; if so, the measured serum exenatide would have underestimated the total released peptide. We note that degradation products in sera would not have been detected with the specific LC-MS/MS exenatide assay used. To estimate an *in vivo* rate of degradation, k_{deg}, of exenatide, eq. 1 was transformed to eq. 2 that describes the C vs t profile of exenatide with concomitant first-order degradation of the peptide bound to the depot.

$$[\text{Drug}]_{CC,t} = \text{Dose} \cdot \frac{F}{CL} \cdot k_1 \cdot (e^{-(k_1+k_{deg})t} - e^{-k_a t}) \qquad [2]$$

After the initial absorption phase, the slope of the $\log[\text{Drug}_{CC}]$ vs t plot becomes

$$k_\beta = k_1 + k_{deg} \qquad [3]$$

and the difference between the observed and expected k_β values for drug release is k_{deg}. Using this approach, the observed vs expected curves in **Fig. 1** can be explained by a first-order destruction of the exenatide tethered to the hydrogel in the SC space with $t_{1/2,deg}$ ~13 days.

Degradation of exenatide. Modification of exenatide on the SC hydrogel could occur by proteolytic or chemical degradation. *A priori*, the former seemed more likely because exenatide

is susceptible to enzymatic degradation [31, 32], and it seemed implausible that a spontaneous chemical degradation of exenatide would have gone unreported to date. Nevertheless, we examined the stability of exenatide under physiological conditions.

We incubated exenatide in 200 mM NaP_i, pH 7.4, 37 °C, and analyzed samples at intervals by HPLC**.** As shown in **Fig 2A,** the exenatide peak disappeared as another developed at a similar retention volume (RV), and two slower eluting peaks emerged; two additional small peaks appeared at later times. At 56 days, the three major products had, in order of their RVs, estimated relative peak areas of ~36, 12 and 46. **Fig. 2B** shows the time-dependent changes of the peak areas of exenatide and two of the three major products. Taken together, these data show that exenatide is degraded with a $t_{1/2}$ of ~10 days under the study conditions.

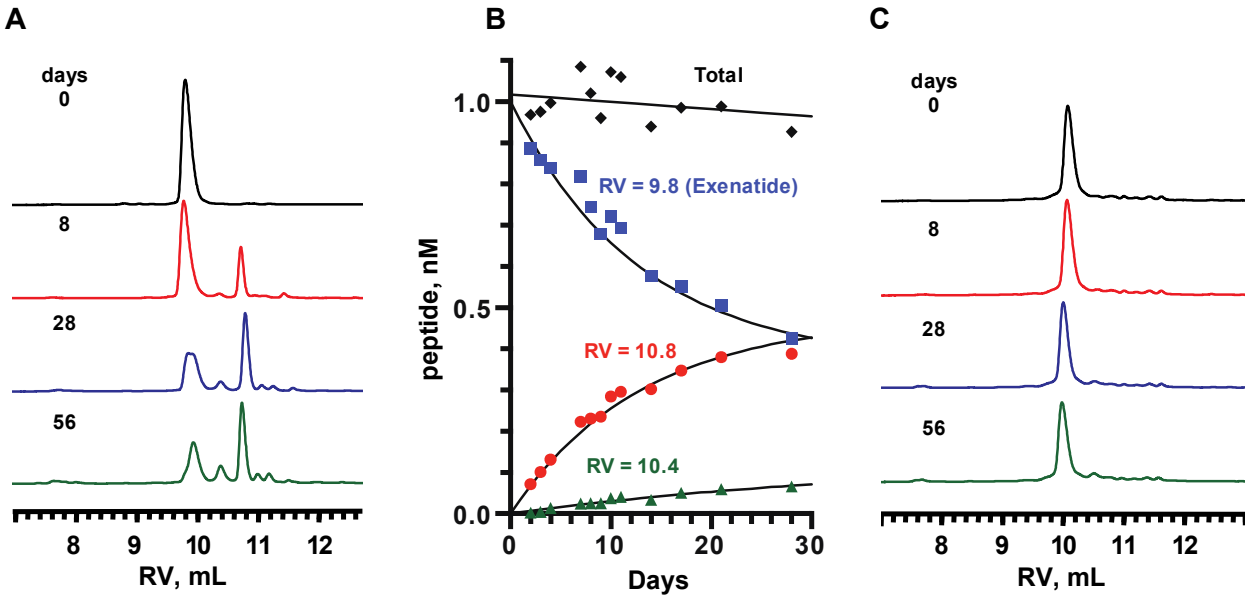

Figure 2. Exenatide and [Gln^{28}]exenatide stability in 200 mM NaP_i, pH 7.4, 37 °C. A. HPLC traces at 0, 8, 28 and 56 days showing exenatide (top) converting to products (bottom). B. Time course of exenatide (-■-, RV 9.8 mL) degradation ($t_{1/2}$ ~10 days) and formation of new products with RV=10.4 (-⑩-; $t_{1/2}$ ~5 wks) and 10.8 (-③-; $t_{1/2}$ ~10 days) mL; the total peak area (-◆-) decreased ~ 5% over 28-days. The rate of formation of the product at RV 9.9 could not be measured and the two minor, latest-appearing peaks had $t_{1/2}$ ~24 days (not shown). The reaction rates were estimated by plots of $\ln[1-(C/C_{inf})]$ vs time for products and $\ln(C/C_{inf})$ vs time for loss of exenatide; C_{inf} values were estimated by optimizing the RMS of the linearity of such plots. C. HPLC traces of [Gln^{28}]exenatide at 0 (top), 8, 28 and 56 (bottom) days. Peak areas were determined as a ratio of A_{280} to 200 μM of H-Lys(DNP)OH as an internal standard.

Product identification. Exenatide has an AsnGly dipeptide in positions 28-29, a sequence that is particularly susceptible to Asn deamidation [33-35]. This well-studied reaction proceeds through formation of an unsymmetrical cyclic imide, which undergoes hydrolysis and isomerization to first give L-isoAsp and L-Asp, and later their D-isomers.

Exenatide: HGEGTFTSDLSKQMEEEAVRLFIEWLK**N^{28}G**GPSSGAPPPS-NH_2

Following is evidence that Asn^{28} deamidation is the major source of exenatide degradation. First, as shown in **Fig. 2C** and below, replacement of Asn^{28} by other amino acid residues

prevented degradation, showing that other residues of exenatide are stable under the study conditions and localizing the degradation of exenatide to Asn^{28}. Second, each of the three major products showed $[M+H]^+$ = 4184.9 Da by ESI-MS, one mass unit higher than exenatide and consistent with the replacement of an amide NH_2 by an OH. The earliest eluting product peak (RV 9.9) co-elutes with synthetic [L-Asp^{28}]exenatide and is not a substrate for protein L-isoAsp methyltransferase (PIMT). The slow-eluting peak (RV 10.8 mL) is [L-isoAsp^{28}]exenatide since, as with deamidation of other AsnGly peptides, it is the largest peak and a substrate for PIMT. Based on relative formation rates in deamidation of other AsnGly peptides, and the absence of PIMT activity, the middle peak (RV 10.4) likely contains [D-isoAsp^{28}]exenatide. Taken together, these results conclusively show that Asn^{28} deamidation is the cause of *in vitro* degradation of exenatide.

When the mixture of degradation products (**Fig. 2A**, t= 56 days) was tested in a cell-based GLP-1R assay in the agonist mode, it had a higher EC_{50} than exenatide (**Fig. S2; Table S2**); isolated [IsoAsp]^{28}- and synthetic [Asp]^{28}exenatides showed EC_{50} values ~2- to 4-fold higher than exenatide.

Deamidation of AsnGly in peptides is general-base catalyzed at near-neutral pH, with the rate dependent on buffer composition and concentration [36]; P_i is a more effective catalyst than sulfonate, and at 20 mM sulfonate Asn deamidation rates are near the unbuffered rate. We examined deamidation rates of exenatide in 20- to 200 mM NaP_i and HEPES buffers at pH 7.4, 37 °C. At comparable concentrations, deamidation rates of exenatide were ~2- to 4-fold faster in P_i than sulfonate; half-lives of deamidation ranged from 10 days in 200 mM P_i to 5 weeks in 20 mM HEPES.

Design of stable exenatide analogs. We sought to modify the Asn^{28}Gly dipeptide of exenatide in a manner that would retain potent GLP-1R agonism but prevent deamidation. The latter can be accomplished by substituting either Asn or Gly by a number of amino acids that provide stable dipeptide sequences [33]. Our choice of which amino acid to substitute and what substitutions to make were influenced by the following considerations.

In the 3-D structure of the exenatide-GLP-1R complex, the side chain of Asn^{28} is exposed to the solvent without contact to the receptor [37]. In contrast, Gly^{29} is in contact with GLP-1R and has a rare +97° Phi dihedral angle. We avoided changing Gly^{29} because a change might perturb important interactions with the receptor and/or the peptide backbone conformation, and because it – but not Asn^{28} – is a known epitope for exenatide-induced antibodies in humans [38].

We chose Gln as a substitute for Asn^{28} because of its high structural similarity and less prone towards deamidation [33]. We also chose Ala, Asp and Lys modifications since they are the most frequent substitutions for Asn at structurally equivalent positions in related proteins [39].

We prepared the Ala, Asp, Gln and Lys substitutions for Asn^{28} of exenatide by SPPS. All [Xaa^{28}]exenatides had EC_{50} values (17- to 41 pM) comparable to exenatide (17 pM) in a GLP-1RA assay (**Fig. S1**). Upon extended incubation (~3 months) of these [Xaa^{28}]exenatides in 200 mM P_i, pH 7.4, 37 °C, major new peaks were not observed, except for [Asp^{28}]exenatide which slowly isomerized to [isoAsp^{28}]exenatide [34]. At low peptide concentrations (~0.2 mM), we observed small loses in A_{280} consistent with non-specific adsorption to vessel surfaces [40]. At 2 mM [Gln^{28}]exenatide, we estimated that the $t_{1/2}$ for loss of peptide was 30 weeks. Hence, [Gln^{28}]exenatide is very stable under physiological conditions.

GLP-1R activation, pharmacokinetics and glucoregulatory effects of [Gln^{28}]exenatide. We chose

[Gln^{28}]exenatide for further study because its high structural similarity to exenatide suggested it is most likely to be similar in pharmacokinetic and pharmacodynamic properties, and least likely to have off-target effects or generate additional antibodies; the additional -CH_2- group only represents a 0.3% increase in MW over exenatide.

Fig. 3 shows that exenatide and [Gln^{28}]exenatide have identical agonist activity in a cell-based GLP-1R assay. Further, the EC_{50} of [Gln^{28}]exenatide was unchanged after 8 wks, demonstrating its stability as an agonist.

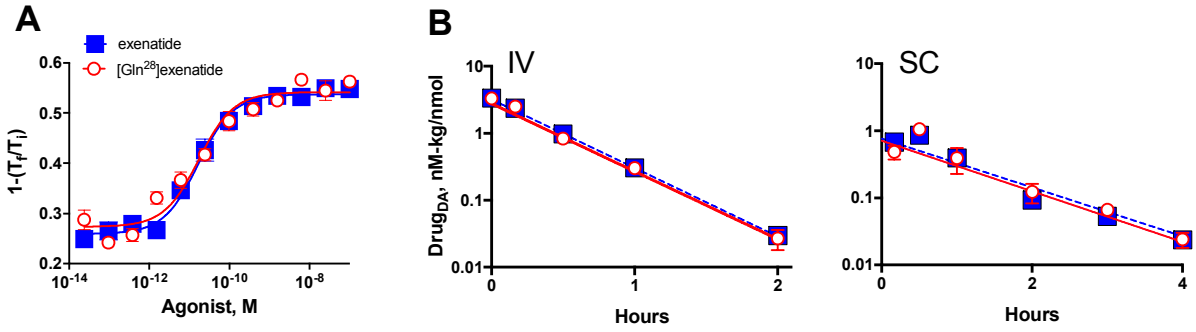

Figure 3. GLP-1RA activity and dose-adjusted C vs t plots of exenatide and [Gln^{28}]exenatide in the rat. A) Comparison of exenatide (-⑤-) and [Gln^{28}]exenatide (-O-) in a cell-based hGLP-1R melanophore assay in agonist mode. T_i and T_f are initial and final response reads, respectively; EC_{50} exenatide = 17 pM, [Gln^{28}]exenatide = 17 pM. Points are averages ± SEM and data were fit to a three-parameter logistic model (solid lines). B) Dose-adjusted C vs t plots of serum peptides after IV (left panel) and SC (right panel) injections of 80 µg/kg exenatide (- -⑤- -) and 50 µg/kg of [Gln^{28}]exenatide (-O-) in the rat; dose adjustments made by dividing serum concentration by dose. Error bars are ±SEM (n=3/group) which are not drawn if bars are shorter than the symbol. There were insufficient early time-points to model distribution or absorption phases.

We compared the pharmacokinetics of [Gln^{28}]exenatide and exenatide in the rat and mouse. Whether administered IV or SC, the dose-adjusted pharmacokinetics of [Gln^{28}]exenatide and exenatide in the rat are indistinguishable (**Fig. 3B; Table S3**). As reported for exenatide [30], the data for SC administration of both peptides are consistent with a flip-flop mechanism with rate-determining absorption having a $t_{1/2}$ of 50 min, followed by an elimination phase with $t_{1/2}$ of 18 min. The dose adjusted AUCs for IV and SC exenatide and [Gln^{28}]exenatide gave SC bioavailabilities of 62-69% (**Table S3**), comparing well to 65-75% reported for exenatide [30]. In the mouse, we obtained $t_{1/2,\beta}$ of 20 min for SC injection identical to that reported for exenatide (**Fig. S4**). Thus, the pharmacokinetic parameters of [Gln^{28}]exenatide and exenatide in rodents were indistinguishable.

We next compared the acute glucoregulatory effects of [Gln^{28}]exenatide and exenatide in the mouse. The peptides were administered as single SC injections to non-diabetic C57BL/6 mice 30 min prior to an oral glucose tolerance test (OGTT) and blood glucose and insulin were measured over the subsequent 6 hrs (**Fig. 4A,B**). Increasing amounts of either [Gln^{28}]exenatide or exenatide caused nearly identical decreases in glucose excursions. The glucose lowering after 30 min by [Gln^{28}]exenatide was identical to that for exenatide (ED_{50} = 0.08 µg/kg) (**Fig. 4C**). Likewise, the dose-dependent decrease of AUC for blood glucose over the study period for [Gln^{28}]exenatide and exenatide were the same (**Fig 4D**). Finally, there was a rise in insulin 15 min after the glucose load that peaked at ~0.3- to 1 µg/kg [Gln^{28}]exenatide or exenatide and then decreased with higher concentrations to give a bell-shaped curve as reported for exenatide

[41, 42] (**Fig. S6**). Thus, the acute glucoregulatory and insulinotropic effects of [Gln^{28}]exenatide and exenatide were identical.

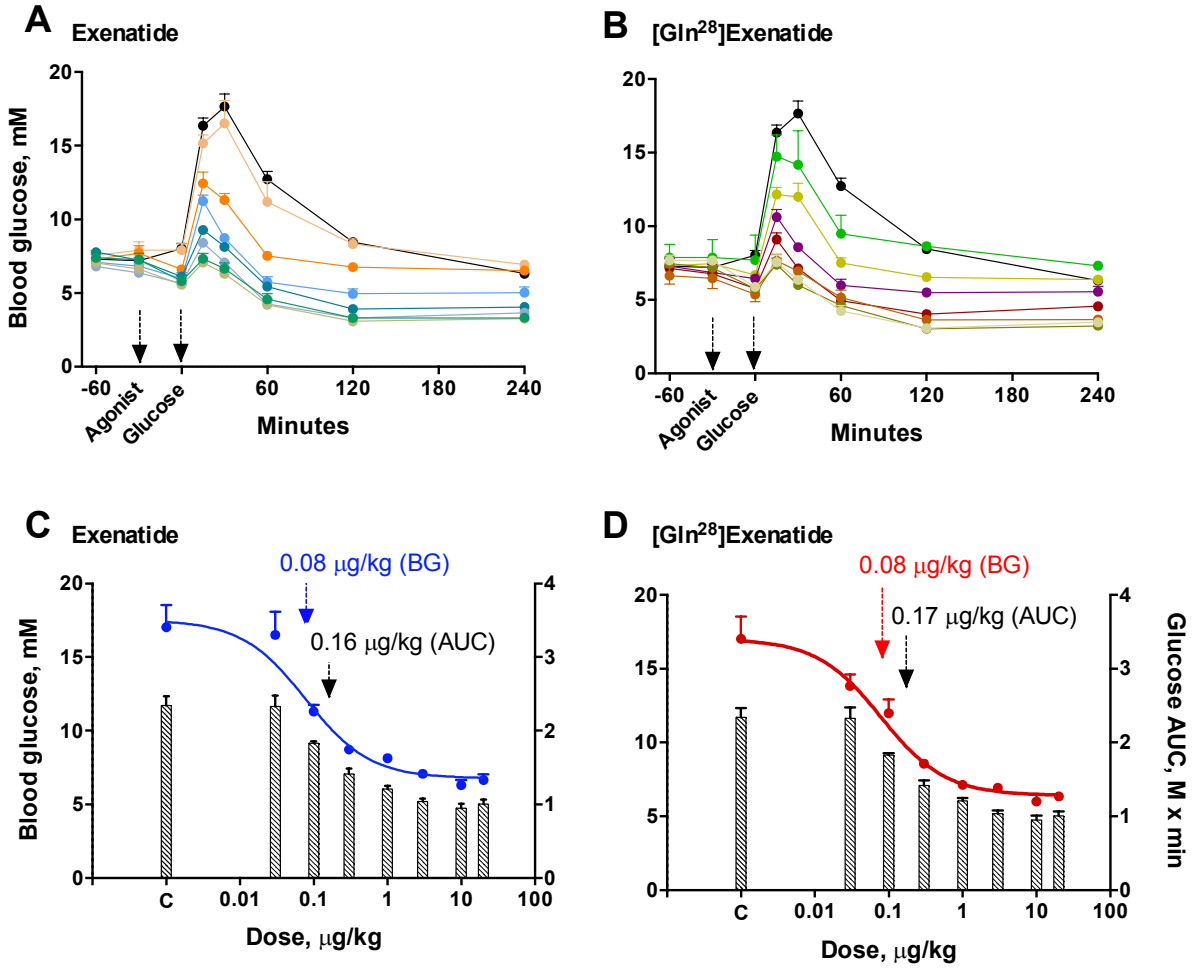

Figure 4. Acute glucose-lowering effects of exenatide and [Gln^{28}]exenatide in C57BL/6 mice. Blood glucose vs time after administration of A) exenatide or B) [Gln^{28}]exenatide 30 min prior to an OGTT; agonist doses are 0 (top), 0.03, 0.1, 0.3, 1, 3, 10 and 20 (bottom) µg/kg. Data from panels A and B are used to construct dose response curves (line) of blood glucose vs C) exenatide dose, ED_{50}= 0.08 µg/kg, or D) [Gln^{28}]exenatide, ED_{50}= 0.08 µg/kg, 30 min after glucose administration; bars show glucose AUC at 4 hrs after glucose administration for C) exenatide, ED_{50}=0.16 µg/kg or D) [Gln^{28}]exenatide ED_{50}= 0.17 µg/kg. Values used for ED_{50} calculations were statistically different from vehicle as shown by two-way RM ANOVA vs vehicle, $p<0.05$, Bonferroni post hoc test. Error bars show +SEM (n=6 mice/group).

Hydrogels with releasable [Gln^{28}]exenatide. [Gln^{28}]exenatide-microspheres were prepared as described for analogous exenatide conjugates [28]. Accelerated release studies of conjugates with $MeSO_2$- and -CN modulators in the linkers gave estimated $t_{1/2}$ values of 620 and 1980 hr, respectively, at pH 7.4, 37 °C. The crosslinks of these microspheres also contained self-cleaving linkers tuned to degrade the polymer after drug release [43].

Microspheres were injected SC into normal rats, and [Gln^{28}]exenatide in serum was measured by LC-MS/MS (**Fig. 5**). The hydrogel using the $MeSO_2$- modulator showed a $t_{1/2,\beta}$ of 13 days, and that with the -CN modulator showed a $t_{1/2,\beta}$ of 37 days, some 1.5- to 3.7-fold longer than

corresponding exenatide conjugates (**Fig.1** and ref. [28]). A pharmacokinetic study of these microspheres in the mouse gave slightly shorter $t_{1/2,\beta}$ values of serum [Gln^{28}]exenatide of 10 and 30 days for the $MeSO_2$- and -CN modulators, respectively (**Fig. S5, Table S4**). The 95% confidence levels for the $t_{1/2,\beta}$ values of the -CN linker in the mouse (24.6- to 40.5 days) and rat (27.4- to 56.2 days) are extensively overlapping, as are those for the $MeSO_2$- linker (7.7- to 15.1 days in mouse vs 11.1- to 15.6 days in rat). In the absence of strong statistical evidence for difference, we use the $t_{1/2,\beta}$ of the linkers in the rat in the ensuing analyses and discussion.

If we assume the pharmacokinetics of the hydrogel-exenatide and [Gln^{28}]exenatide conjugates differ only because of the deamidation of the former, we can estimate the rate of *in vivo* deamidation, k_{deg}, using eq. 1 to obtain k_1 for [Gln^{28}]exenatide, eq. 2 to obtain $k_1 + k_{deg}$ for exenatide and then solving for k_{deg} in eq. 3. From this, we estimate the *in vivo* $t_{1/2}$ values of deamidation of exenatide in the rat as 14 days for either linker. This value is in excellent accord with the estimated $t_{1/2,deg}$ for exenatide deamidation of ~13 days from the simulated expected and experimentally observed $t_{1/2,\beta}$ values of the hydrogel-exenatide conjugate obtained at the outset of this study (**Fig. 1**).

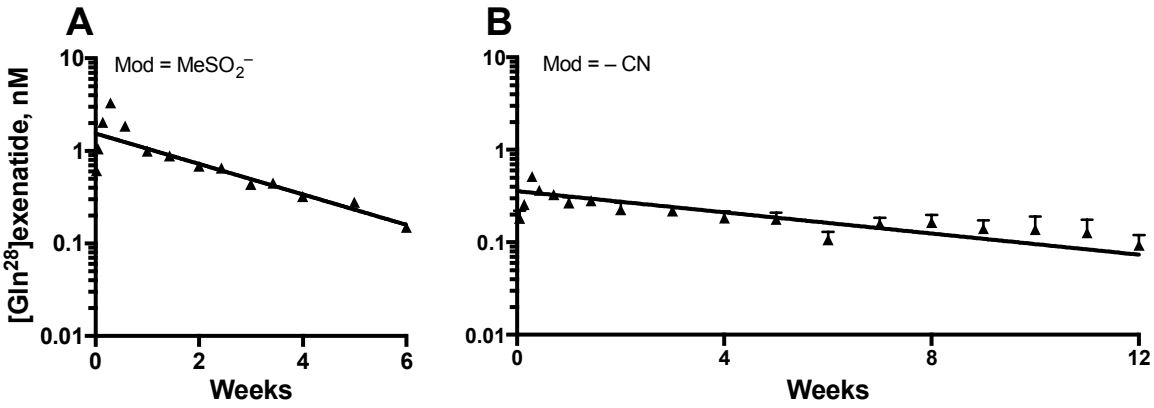

Figure 5. Serum [Gln^{28}]exenatide levels after SC injection of rats with microsphere conjugates. A) After injection with [Gln^{28}]exenatide microspheres with a $MeSO_2$- modulator (0.17 µmol [Gln^{28}]exenatide/rat, 2.6 mg [Gln^{28}]exenatide/kg); $t_{1/2,\beta}$ was 310 hr. B) After injection with hydrogel-[Gln^{28}]exenatide microspheres with a -CN modulator (0.6 µmol [Gln^{28}]exenatide/rat, 8.9 mg [Gln^{28}]exenatide/kg); $t_{1/2,\beta}$ was 880 hr. Early time points were insufficient to calculate absorption phase kinetics, and were not used in fitting the β-phase shown. Error bars are +SEM (n=6 rats/group). Analogous experiments in the mouse are provided in **Fig. S5**.

Eight-week pharmacodynamic effects of once-monthly administered [Gln^{28}]exenatide microspheres. The male Zucker diabetic fatty (ZDF) rat – a widely used model for obese T2D in humans [44] – develops diabetes between 6 and 10 weeks of age when fed a high fat diet and undergoes a progressive deterioration of beta-cell function in the face of insulin resistance. After the onset of disease, they show signs of T2D such as hyperglycemia, insulin resistance, increased food and water intake, weight gain, and increased gastric emptying rate; they also show diminished glucose lowering and insulin responses when challenged with glucose in an OGTT, and increased HbA1c after prolonged hyperglycemia. Continuous exposure to GLP-1RAs improves most of these diabetic pathological changes [1, 45].

We compared the 8-week pharmacodynamic effects of the long-acting releasable microsphere-[Gln^{28}]exenatide (Mod= -CN) with continuously infused-exenatide (CI-exenatide) in 8 week old

male ZDF rats. Eligible rats were stratified into 4 groups (10/group) based on morning fed blood glucose, and individual groups received: a) Alzet pump vehicle control (50 mM NaOAc, pH 4.5); b) Alzet pump with 0.2 µg/mL exenatide in vehicle delivered at 30 µg/kg/day; c) QM injections of SC microsphere-[Gln^{28}]exenatide at 920 µg and d) 9200 µg/kg along with vehicle control pumps. The dose of CI-exenatide and the lower dose of [Gln^{28}]exenatide microspheres were both targeted to give a C_{min} of ~ 0.1 nM serum peptide, and the higher dose of [Gln^{28}]exenatide microspheres at C_{min} of 1 nM. After 4-weeks, pumps were replaced, and rats were re-injected with [Gln^{28}]exenatide-microspheres at the same doses.

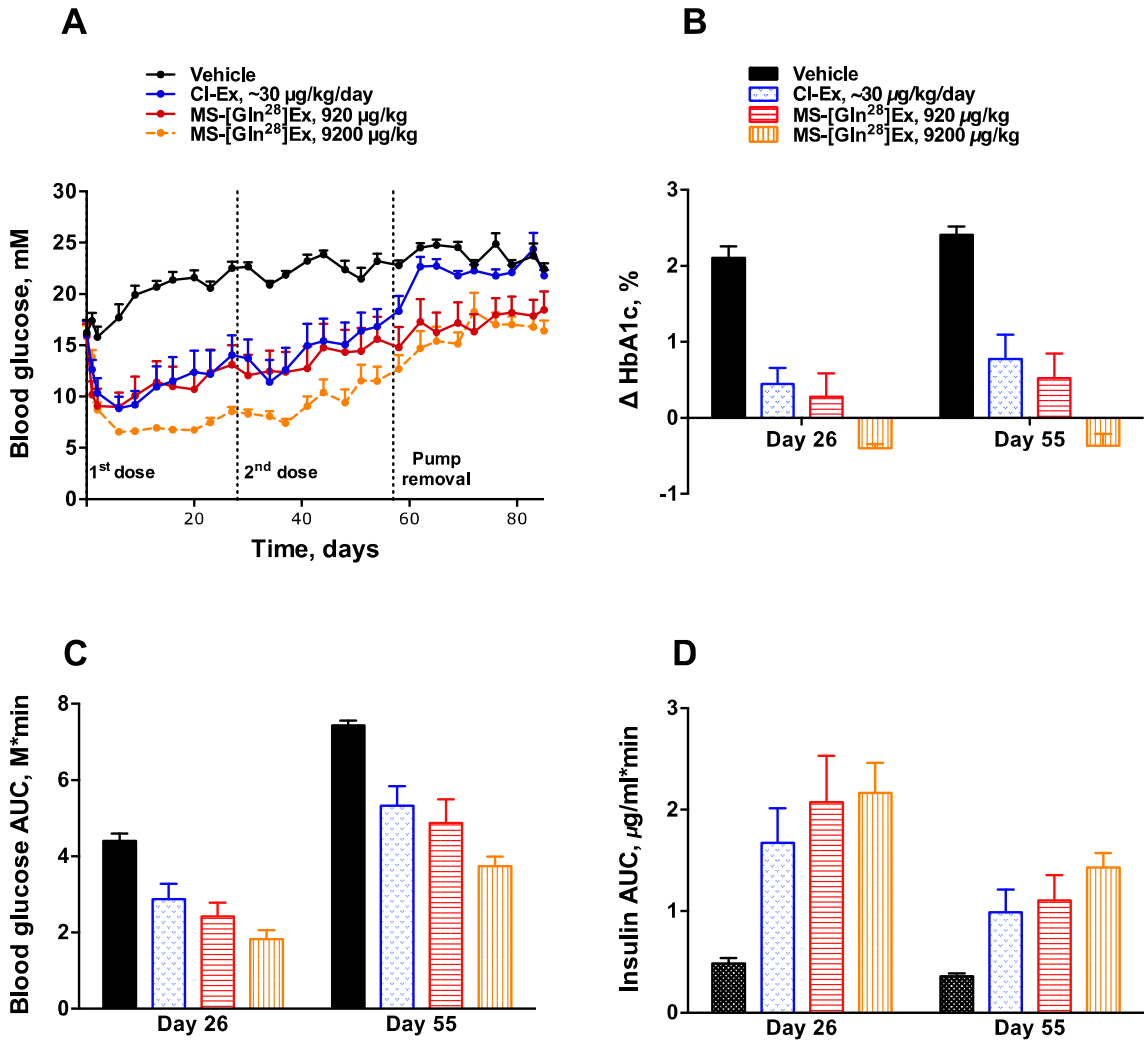

Figure 6. Effects of two monthly SC injections of [Gln^{28}]exenatide-microspheres *vs* CI-exenatide on glucose homeostasis in diabetic male ZDF rats. Effects on (A) blood glucose levels (morning fed glucose), B) HbA1c levels at days 26 and 55. At days 26 and 56 OGTTs were performed measuring (C) blood glucose and (D) insulin AUC values. Bar graph columns represent vehicle control (solid), 30 ug/kg/day CI-exenatide (dotted), 920 µg/kg (horizontal lines) and 9200 µg/kg (vertical lines) [Gln^{28}]exenatide-microspheres. Data show mean +SEM (n=10 mice/group). Data analyzed by one-way ANOVA (bar-graphs) or two-way repeated measures ANOVA (line-graphs) with Bonferroni post-hoc test. * p<0.05, ** p<0.01, *** p<0.001.

All studied pharmacodynamic effects of two monthly SC injections of 920 µg/kg microsphere-[Gln^{28}]exenatide closely tracked those of 30 ug/kg/day CI-exenatide (**Table 1**, **Figs. 6** and **S7)**; expectedly, the 10-fold higher dose of [Gln^{28}]exenatide-microspheres showed more pronounced anti-diabetic effects. Analyses of serum peptides at eight weekly intervals gave C vs t plots very close to what was anticipated (**Fig. S8**); the data showed C_{ave} of 0.13 and 1.2 nM for the low and high doses of microsphere-[Gln^{28}]exenatide, respectively, and 0.17 pM for exenatide CI.

Animals treated with CI-exenatide and microsphere-[Gln^{28}]exenatide showed a rapid decrease in blood glucose that persisted over the 8-wk study period albeit with the slow, consistent rise as the ZDF rats become more diabetic (**Fig. 6A; Table 1**). The glucose-lowering effects translated into significant reduction of HbA1c levels – a measure of cumulative blood glucose levels – compared to untreated animals on days 26 and 55 (**Fig. 6B**); notably, the higher dose of [Gln^{28}]exenatide-microspheres actually decreased HbA1c levels below pre-treatment levels. Both CI-exenatide and [Gln^{28}]exenatide-microspheres reduced food and water intake over the entire study period in a manner characteristic of continuous exposure of ZDF rats to GLP-1RAs [45, 46](**Table 1, Fig. S7**). Initially, treated animals showed a rapid weight loss; after ~3 days, weight gain increased and after ~4 weeks the weights of treated rats exceeded that of controls (**Fig. S7**). Despite hyperphagia, body weight gain of severely diabetic ZDF rats is impacted by significant loss of calories via glucosuria [44]; ZDF rats treated with a long-acting GLP-1RA show improved diabetes and may not suffer this caloric loss, resulting in paradoxical weight gain despite lower food intake [45].

Table 1. Relative cumulative food and water intake, and average blood glucose over the 8 week study period in the ZDF rat.[A]

	Vehicle	CI-exenatide (30 µg/kg/day)	MS-[Gln^{28}]Ex (920 µg/kg)	MS-[Gln^{28}]Ex (9200 µg/kg)
Food Intake	100 ±2	74 ±4	68 ±4	55 ±2
Water Intake	100 ±6	51 ±9	42 ±8	25 ±1
Blood glucose	100 ±2	64 ±8	57 ±9	40 ±2

[A] The values of serial data of treated animals (**Fig. S7**) were determined over 8 weeks and are expressed as the percent of that observed in the vehicle control.

In the OGTT performed on days 26 and 56, treated animals showed significantly improved glucose responses and AUC values, together with a greater insulin secretory response (**Figs. 6C,D, S7**). The robust anti-hyperglycemic and insulinotropic effects of the [Gln^{28}]exenatide-microspheres persist throughout the 8-week treatment period and indicate preservation of beta-cells. Lastly, there was no difference between treated and untreated rats in gastric emptying rate (**Fig. S7**), in accord with the desensitization of acute inhibition that is observed after continuous exposure to GLP-1RAs [47].

After the study period, pumps were removed and animals were maintained for four additional weeks. Because of the short $t_{1/2,\beta}$ of exenatide, glucose levels, as well as food and water intake of rats withdrawn from CI-exenatide rapidly reverted to control levels (**Figs. 6A, S7**). Rats treated with [Gln^{28}]exenatide-microspheres reverted more slowly since the drug-releasing depot remained in the animals. HbA1c levels at day 85 likewise reflected the rapid reversion of animals treated with CI-exenatide, and slower reversion of rats treated with extended-release [Gln^{28}]exenatide-microspheres.

In summary, the above results convincingly demonstrate that in the diabetic ZDF rat model of T2D, the chronic pharmacodynamic effects of once-monthly injected [Gln^{28}]exenatide

microspheres are dose dependent and indistinguishable from those observed with continuous exposure to native exenatide.

Pharmacokinetic simulations in the human. We previously described an approach for inter-species modeling of the pharmacokinetics of drugs released from β-eliminative linkers attached to non-circulating carriers [28]. The simulation requires knowledge of the linker cleavage rate, which, although not yet determined in humans, are chemically-controlled and apparently species-independent [25, 48]. Notably, the serum $t_{1/2,\beta}$ values of [Gln^{28}]exenatide released from the two microsphere conjugates studied here are, within experimental error, the same in the mouse and rat.

Eq. 4 describes the steady state dose needed to maintain the drug concentration above a therapeutic minimum concentration C_{min} for a specified interval, t_{min} [28].

$$Dose_{ss} = C_{min} \cdot \frac{CL}{F \cdot k_1} \cdot (e^{k_1 t_{min}} - 1) \qquad [4]$$

For dosage estimations in humans, we calculated CL of exenatide as 0.123 L/hr/kg from $CL=Dose_{SS}/C_{SS}/BW$ using the results of 25 ng/min CI-exenatide [49]. From this, and the V_d of 0.4 L/kg and F=1 (Byetta package), we estimated an elimination $t_{1/2,\beta}$ of 2.3 hr, in excellent agreement with the 2.4 hr $t_{1/2,\beta}$ for SC injection (Byetta label). Although analogous values for [Gln^{28}]exenatide in the human are not known, we justify using those of exenatide because of the high structural similarity and the near-identical GLP-1R EC_{50} values, pharmacokinetics and *in vivo* glucoregulatory effects in rodents. We targeted the exenatide therapeutic C_{min} of ~70 pM that is achieved with a 2 mg weekly-dose Bydureon [50, 51], calculated the dose from eq. 4 and estimated the C_{max} and steady state AUC from superposition of single dose C vs t plots (eq. 1).

Simulated steady state parameters of drug released from hydrogel-exenatide and [Gln^{28}]exenatide conjugates are compared in **Table 2**. QW Bydureon serves as a comparator and its reported C_{max} and C_{max}/C_{min} values serve as guidance for limits known to be tolerable. We also show values for continuous infusion of 60 μg/day exenatide *via* the Medici™ implantable pump drug delivery system that achieves a constant ~70 pM concentration and represents the lowest efficacious dose and the most efficient AUC that maintains the therapeutic C_{min} [24]. Higher AUC values of other delivery systems represent "wasted" exposure.

The previously reported QW exenatide conjugate $t_{1/2,\beta}$ of ~7 days for released exenatide [28] would require a high dose to span the four half-lives needed to support QM administration, and have unacceptably high C_{max} and C_{max}/C_{min} values compared to Bydureon. With the CN modulator, the $t_{1/2,\beta}$ of released exenatide increases to 240 hrs, but with an estimated deamidation $t_{1/2}$ of ~14 days (**Fig. 1**) is unsuitable for QM dosing.

[Gln^{28}]exenatide microspheres with a $MeSO_2$- modulator has a $t_{1/2,\beta}$ for the released peptide that would be suitable for biweekly administration, but not for QM administration because the C_{max}/C_{min} would be ~3-fold higher than weekly Bydureon. With the -CN modulator and [Gln^{28}]exenatide, the $t_{1/2,\beta}$ is a very long 37 days, and should maintain the drug serum levels ≥C_{min} with only ~2.6 mg of peptide/month, while maintaining a C_{max} and C_{max}/C_{min} that is similar to that for each QW Bydureon dose. As measured by the AUC the efficiency of drug utilization was 75% of the near-perfect CI-exenatide. It would take ~12 weeks for the [Gln^{28}]exenatide to reach steady state, which is not much longer than the 8- to 10 weeks needed for QW Bydureon. However, by administering a loading dose twice the steady state dose, and initiating monthly

injections at week 3, the steady state C_{min} would be reached by day 2 and the steady state C_{max} would never be exceeded. We note that this conjugate would require a monthly injection of less than 0.5 mL of microspheres which contains ~4 mg exenatide.

Table 2. Reported and simulated steady state pharmacokinetic parameters of exenatide and [Gln^{28}]exenatide released from delivery systems in humans.

Drug (Modulator)	**Dosing interval**	**Serum exenatide or [Gln^{28}]exenatide**					
		dose, mg/mo (wk) [A]	**$t_{1/2,\beta}$, hr**	**C_{min}, nM**	**C_{max}, nM**	**C_{max}/C_{min}**	**AUC nM-hr/wk**
Bydureon [B]	QW	8 (2)	NA	0.07	0.12	1.7 [C]	57
CI-exenatide (ITCA 650)	–	1.7 (0.42)	NA	0.07	0.07	1.0	12
MS-exenatide ($MeSO_2$-)	QM	10.4 [D]	160	0.07	1.31	18.7	74
MS-exenatide (-CN)	QM	5.4 [D]	240	0.07	0.51	7.2	38
MS-[Gln^{28}]exenatide ($MeSO_2$-)	QM	4.2 [D]	310	0.07	0.33	4.7	29
MS-[Gln^{28}]exenatide (-CN)	QM	2.6 [D]	880	0.07	0.13	1.8	16

[A] One month is assumed to have 28 days. [B] Bydureon PK parameters from Refs [50, 51]. [C] Four excursions per month. [D] Dose values for simulations assume 100% bioavailability of [Gln^{28}]exenatide and exenatide in the human, as it is with SC exenatide (Byetta label).

Discussion

The primary objective of this work was to develop a long-acting GLP-1RA that could be administered by monthly SC injections. Compared to current QW agonists, obvious benefits would be greater patient convenience, compliance and persistence. A longer-acting agonist would also allow advancing or delaying a dose a short period, and lessen the burden of caregivers responsible for drug administration to reliant patients. Therapeutic benefits could as well be realized after QM GLP-1RAs are validated and have undergone appropriate clinical studies.

The approach we used was to tether a GLP-1RA to a hydrogel microsphere depot by a self-cleaving β-eliminative linker with a pre-programmed cleavage rate; upon subcutaneous injection the linker slowly cleaves and releases the drug into the systemic circulation. We previously used this approach to prepare a hydrogel-exenatide conjugate that should support weekly administration in the human [28].

In preliminary work, we attempted to increase the duration of exenatide exposure by using a slower-cleaving linker, but found a less than expected $t_{1/2,\beta}$ and exposure. We speculated that the unexpected pharmacokinetic result was due to degradation of the hydrogel-bound peptide, and found that exenatide undergoes spontaneous deamidation at Asn^{28}, which we estimated would have a half-life of ~14 days *in vivo*. The deamidation products – Asp and isoAsp-containing peptides – are agonists of the GLP-1R, but were not detectable in the assays used for serum exenatide. Although it is possible these products would not greatly affect the

pharmacological activity, we elected to avoid degradation products rather than study them. Parenthetically, a similar deamidation of Asn[28] is likely to occur in other long-acting GLP-1 agonists that have exenatide-related sequences containing an AsnGly dipeptide [22, 52].

We subsequently showed that substitution of Asn[28] by several other amino acid residues stabilizes the peptide while maintaining excellent agonist activity for hGLP-1R. We selected [Gln[28]]exenatide for further study because its close structural similarity to exenatide – a single methylene group difference – suggested it should be most analogous in pharmacokinetic and pharmacodynamic properties, and least likely to generate off-target effects or additional antibodies. We showed that [Gln[28]]exenatide has identical GLP-1RA activity, pharmacokinetics and glucoregulatory effects as native exenatide, but does not suffer the instability of the parent peptide.

We attached [Gln[28]]exenatide to hydrogel microspheres via two different β-eliminative linkers previously used in analogous exenatide conjugates, injected the microspheres SC in the mouse and the rat, and measured serum [Gln[28]]exenatide over time. Pharmacokinetic analyses showed serum half-lives of about two weeks and one month for the released [Gln[28]]exenatide. Two monthly administrations of the longer-acting [Gln[28]]exenatide-microspheres in the rat showed identical pharmacodynamic effects as continuously infused exenatide over the same period.

Pharmacokinetic simulations indicated that the conjugate with a $t_{1/2,\beta}$ of about one month would favorably support once-monthly administration in humans. It should maintain a continuous therapeutic serum concentration with monthly C_{max} and C_{max}/C_{min} values comparable or lower than those of currently available QW GLP-1 agonists. The QM [Gln[28]]exenatide-microsphere formulation has other desirable features: a) it can be injected SC in a small volume through a small bore 27- to 30-gauge needle; b) it can be stored for long periods as a slightly-acidic liquid suspension of microspheres amenable for use in a pre-filled auto-injection device; c) it does not require reconstitution of components before self-administration; and d) significantly reduced costs should be realized since the delivery system requires less frequent dosing than current formulations.

In summary, we have developed a novel drug delivery system for a peptidic GLP-1RA that is a viable candidate for once-monthly SC administration for treatment of Type 2 diabetes. The [Gln[28]]exenatide-microspheres could provide a new option for T2D patients that desire a longer dosing interval than current QW formulations, but are reluctant to have an osmotic pump surgically implanted that can deliver a GLP-1RA over a longer duration.

Materials and Methods

The source of specialized materials is provided along with their use in SI. Detailed synthetic, conjugation and analytical procedures are described. *In vitro* kinetic procedures are provided as are *in vivo* pharmacokinetic and pharmacodynamics methods and analyses.

Supplementary Material

Materials and Methods
Figure S1. hGLP-1R assays of [Xaa[28]]exenatides.
Figure S2. GLP-1R bioassays of exenatide and its degradation products.
Figure S3. IsoAsp determinations in exenatide degradation.
Figure S4. C vs t of serum exenatide and [Gln[28]]exenatide in mice.
Figure S5. Serum [Gln][28]exenatide after SC injection of mice with microsphere conjugates.

Figure S6. Insulin levels of varying doses of exenatide and [Gln^{28}]exenatide in OGTTs.
Figure S7. Three month pharmacodynamic study in ZDF rats.
Figure S8. GLP-1RAs serum levels in ZDF rats.

Table S1. EC_{50} values of synthetic [Xaa^{28}]exenatide in GLP-1R assays.
Table S2. EC_{50} of [Asp^{28}]exenatide and exenatide deamidation products
Table S3. Pharmacokinetic parameters of exenatide and [Gln^{28}]exenatide in the rat.
Table S4. Pharmacokinetic properties of [Gln]^{28}exenatide-microspheres.

Acknowledgments: We thank H. Jo and B. Degrado for preparing peptides, M. Mebrahtu for performing the melanophore bioassays and A. Sali for assistance with structural features of the exenatide-GLP-1R interaction. This work was supported in part by NSF grant 1429972.

Author contributions: E.L.S, B.R.H., S.J.P., R.R., N.V., G.W.A. designed and performed experiments and analyzed data. A.L. synthesized drug compounds. D.J.P. and D.V.S. provided methodological and conceptual input and D.V.S. wrote the manuscript.

Competing interests: E.L.S, B.R.H., S.J.P., R.R., N.V., G.W.A., D.J.P. and D.V.S. hold options or stock in the company.

References

1. Madsbad, S. (2016) Review of head-to-head comparisons of glucagon-like peptide-1 receptor agonists, *Diabetes Obes. Metab. 18*, 317-332.

2. Campbell, J. E., and Drucker, D. J. (2013) Pharmacology, physiology, and mechanisms of incretin hormone action, *Cell Metab. 17*, 819-837.

3. Hanna, A., Connelly, K. A., Josse, R. G., and McIntyre, R. S. (2015) The non-glycemic effects of incretin therapies on cardiovascular outcomes, cognitive function and bone health, *Expert Rev. Endocrinol. Metab. 10*, 101-114.

4. Madsbad, S. (2014) The role of glucagon-like peptide-1 impairment in obesity and potential therapeutic implications, *Diabetes Obes. Metab. 16*, 9-21.

5. Potts, J. E., Gray, L. J., Brady, E. M., Khunti, K., Davies, M. J., and Bodicoat, D. H. (2015) The Effect of Glucagon-Like Peptide 1 Receptor Agonists on Weight Loss in Type 2 Diabetes: A Systematic Review and Mixed Treatment Comparison Meta-Analysis, *PLoS One 10*, e0126769.

6. Baggio, L. L., and Drucker, D. J. (2014) Glucagon-like peptide-1 receptors in the brain: controlling food intake and body weight, *J. Clin. Invest. 124*, 4223-4226.

7. Marso, S. P., Daniels, G. H., Brown-Frandsen, K., Kristensen, P., Mann, J. F., Nauck, M. A., Nissen, S. E., Pocock, S., Poulter, N. R., Ravn, L. S., Steinberg, W. M., Stockner, M., Zinman, B., Bergenstal, R. M., Buse, J. B., and Investigators, L. S. C. o. b. o. t. L. T. (2016) Liraglutide and Cardiovascular Outcomes in Type 2 Diabetes, *New Engl. J. Med.*

8. Marso, S. P., Bain, S. C., Consoli, A., Eliaschewitz, F. G., Jodar, E., Leiter, L. A., Lingvay, I., Rosenstock, J., Seufert, J., Warren, M. L., Woo, V., Hansen, O., Holst, A. G., Pettersson, J.,

Vilsboll, T., and Investigators, S.-. (2016) Semaglutide and Cardiovascular Outcomes in Patients with Type 2 Diabetes, *New Engl. J. Med.*

9. Ussher, J. R., and Drucker, D. J. (2014) Cardiovascular actions of incretin-based therapies, *Circul. Res. 114*, 1788-1803.

10. Drucker, D. J. (2016) The Cardiovascular Biology of Glucagon-like Peptide-1, *Cell Metab. 24*, 15-30.

11. Armstrong, M. J., Gaunt, P., Aithal, G. P., Barton, D., Hull, D., Parker, R., Hazlehurst, J. M., Guo, K., team, L. t., Abouda, G., Aldersley, M. A., Stocken, D., Gough, S. C., Tomlinson, J. W., Brown, R. M., Hubscher, S. G., and Newsome, P. N. (2016) Liraglutide safety and efficacy in patients with non-alcoholic steatohepatitis (LEAN): a multicentre, double-blind, randomised, placebo-controlled phase 2 study, *Lancet 387*, 679-690.

12. Parkes, D. G., Mace, K. F., and Trautmann, M. E. (2013) Discovery and development of exenatide: the first antidiabetic agent to leverage the multiple benefits of the incretin hormone, GLP-1, *Expert Opin. Drug Discov. 8*, 219-244.

13. Tibble, C. A., Cavaiola, T. S., and Henry, R. R. (2013) Longer Acting GLP--1 Receptor Agonists and the Potential for Improved Cardiovascular Outcomes, *Expert Rev. Endocrinol. Metab. 8*, 247-259.

14. Polonsky, W. H., and Henry, R. R. (2016) Poor medication adherence in type 2 diabetes: recognizing the scope of the problem and its key contributors, *Patient Prefer. Adherence 10*, 1299-1307.

15. Freemantle, N., Satram-Hoang, S., Tang, E. T., Kaur, P., Macarios, D., Siddhanti, S., Borenstein, J., Kendler, D. L., and Investigators, D. (2012) Final results of the DAPS (Denosumab Adherence Preference Satisfaction) study: a 24-month, randomized, crossover comparison with alendronate in postmenopausal women, *Osteoporosis Int. 23*, 317-326.

16. Tkacz, J., Ellis, L., Bolge, S. C., Meyer, R., Brady, B. L., and Ruetsch, C. (2014) Utilization and adherence patterns of subcutaneously administered anti-tumor necrosis factor treatment among rheumatoid arthritis patients, *Clin. Ther. 36*, 737-747.

17. Kishimoto, H., and Maehara, M. (2015) Compliance and persistence with daily, weekly, and monthly bisphosphonates for osteoporosis in Japan: analysis of data from the CISA, *Arch. Osteoporos. 10*, 231.

18. Zierhut, M. L., and Cirincione, B. B. (2014) Method for treating diabetes with extended release formulation of GLP-1 receptor agonists, *US 2014/0220134 A1*.

19. Wysham, C. H., MacConell, L., and Hardy, E. (2016) Efficacy and Safety of Multiple Doses of Exenatide Once-Monthly Suspension in Patients With Type 2 Diabetes: A Phase 2 Randomized Clinical Trial, *Diabetes Care*.

20. Del Prato, S., Kang, J., Choi, S., Lee, W., Han, O., Kil, S., Gee, K., Choi, I. Y., Kwon, S. C., Trautmann, M., and Hompesch, M. (2015) Once-a-Month Treatment with HM11260C Improves Glycemic Control in Type 2 Diabetes (T2DM)—Interim Data from a 16-Week Study, In *American*

Diabetes Association (ADA) 75th Scientific Sessions, June 5 – 9, Boston, Massachusetts. , pp Abstract 105-LB.

21. Rosenstock, J., Reusch, J., Bush, M., Yang, F., Stewart, M., and Albiglutide Study, G. (2009) Potential of albiglutide, a long-acting GLP-1 receptor agonist, in type 2 diabetes: a randomized controlled trial exploring weekly, biweekly, and monthly dosing, *Diabetes Care 32*, 1880-1886.

22. Podust, V. N., Balan, S., Sim, B. C., Coyle, M. P., Ernst, U., Peters, R. T., and Schellenberger, V. (2015) Extension of in vivo half-life of biologically active molecules by XTEN protein polymers, *J. Controlled Release*.

23. Cleland, J., Aronson, R., Humphriss, E., Shore, C. R., Bright, G., Zhou, R., and Kipnes, M. S. (2012) Safety, pharmacokinetics, and pharmacodynamics of a single subcutaneous dose of VRS-859 in patients with type 2 diabetes, In *European Association for the Study of Diabetes (EASD) 48th Annual Meeting*, pp Abstract #821, S338-S339, Diabetologia, Berlin, Germany.

24. Henry, R. R., Rosenstock, J., Logan, D., Alessi, T., Luskey, K., and Baron, M. A. (2014) Continuous subcutaneous delivery of exenatide via ITCA 650 leads to sustained glycemic control and weight loss for 48 weeks in metformin-treated subjects with type 2 diabetes, *J. Diabetes Complications 28*, 393-398.

25. Santi, D. V., Schneider, E. L., Reid, R., Robinson, L., and Ashley, G. W. (2012) Predictable and tunable half-life extension of therapeutic agents by controlled chemical release from macromolecular conjugates, *Proc. Natl. Acad. Sci. USA 109*, 6211-6216.

26. Ashley, G. W., Henise, J., Reid, R., and Santi, D. V. (2013) Hydrogel drug delivery system with predictable and tunable drug release and degradation rates, *Proc. Natl. Acad. Sci. USA 110*, 2318-2323.

27. Henise, J., Hearn, B. R., Ashley, G. W., and Santi, D. V. (2015) Biodegradable tetra-PEG hydrogels as carriers for a releasable drug delivery system, *Bioconj. Chem. 26*, 270-278.

28. Schneider, E. L., Henise, J., Reid, R., Ashley, G. W., and Santi, D. V. (2016) Hydrogel Drug Delivery System Using Self-Cleaving Covalent Linkers for Once-a-Week Administration of Exenatide, *Bioconj. Chem. 27*, 1210-1215.

29. Schneider, E. L., Hearn, B. R., Pfaff, S. J., Fontaine, S. D., Reid, R., Ashley, G. W., Grabulovski, S., Strassberger, V., Vogt, L., Jung, T., and Santi, D. V. (2016) Approach for Half-Life Extension of Small Antibody Fragments That Does Not Affect Tissue Uptake, *Bioconj. Chem.*, DOI: 10.1021/acs.bioconjchem.1026b00469.

30. Parkes, D., Jodka, C., Smith, P., Nayak, S., Rinehart, L., Gingerich, R., Chen, K., and Young, A. (2001) Pharmacokinetic Actions of Exendin-4 in the Rat: Comparison With Glucagon-Like Peptide-1, *Drug Dev. Res. 53*, 260-267.

31. Chen, J., Yu, L., Wang, L., Fang, X., Li, L., and Li, W. (2007) Stability of synthetic exendin-4 in human plasma in vitro, *Protein Peptide Lett. 14*, 19-25.

32. Liao, S., Liang, Y., Zhang, Z., Li, J., Wang, J., Wang, X., Dou, G., Zhang, Z., and Liu, K. (2015) In vitro metabolic stability of exendin-4: pharmacokinetics and identification of cleavage products, *PLoS One 10*, e0116805.

33. Robinson, N. E., Robinson, Z. W., Robinson, B. R., Robinson, A. L., Robinson, J. A., Robinson, M. L., and Robinson, A. B. (2004) Structure-dependent nonenzymatic deamidation of glutaminyl and asparaginyl pentapeptides, *J. Pept. Res. 63*, 426-436.

34. Geiger, T., and Clarke, S. (1986) Deamidation, Isomerization, and Racemization at Asparaginyl and Aspartyl Residues in Peptides, *J. Biol. Chem. 262*, 785-794.

35. Wakankar, A. A., and Borchardt, R. T. (2006) Formulation considerations for proteins susceptible to asparagine deamidation and aspartate isomerization, *J. Pharm. Sci. 95*, 2321-2336.

36. Tyler-Cross, R., and Schirch, V. (1991) Effects of amino acid sequence, buffers, and ionic strength on the rate and mechanism of deamidation of asparagine residues in small peptides, *J. Biol. Chem. 266*, 22549-22556.

37. Runge, S., Thogersen, H., Madsen, K., Lau, J., and Rudolph, R. (2008) Crystal structure of the ligand-bound glucagon-like peptide-1 receptor extracellular domain, *J. Biol. Chem. 283*, 11340-11347.

38. Fineman, M. S., Mace, K. F., Diamant, M., Darsow, T., Cirincione, B. B., Booker Porter, T. K., Kinninger, L. A., and Trautmann, M. E. (2012) Clinical relevance of anti-exenatide antibodies: safety, efficacy and cross-reactivity with long-term treatment, *Diabetes Obes. Metab. 14*, 546-554.

39. Overington, J., Donnelly, D., Johnson, M. S., Sali, A., and Blundell, T. L. (1992) Environment-specific amino acid substitution tables: tertiary templates and prediction of protein folds, *Protein Sci. 1*, 216-226.

40. Maes, K., Smolders, I., Michotte, Y., and Van Eeckhaut, A. (2014) Strategies to reduce aspecific adsorption of peptides and proteins in liquid chromatography-mass spectrometry based bioanalyses: an overview, *J. Chromatogr. 1358*, 1-13.

41. Parkes, D. G., Pittner, R., Jodka, C., Smith, P., and Young, A. (2001) Insulinotropic actions of exendin-4 and glucagon-like peptide-1 in vivo and in vitro, *Metabolism 50*, 583-589.

42. Cao, Y., Gao, W., and Jusko, W. J. (2012) Pharmacokinetic/pharmacodynamic modeling of GLP-1 in healthy rats, *Pharm. Res. 29*, 1078-1086.

43. Reid, R., Sgobba, M., Raveh, B., Rastelli, G., Sali, A., and Santi, D. (2015) Analytical and Simulation-Based Models for Drug Release and GelDegradation in a Tetra-PEG Hydrogel Drug-Delivery System, *Macromolecules 48*, 7359-7369.

44. Shiota, M., and Printz, R. L. (2012) Diabetes in Zucker diabetic fatty rat, *Methods Mol. Biol. 933*, 103-123.

45. Gedulin, B. R., Smith, P., Prickett, K. S., Tryon, M., Barnhill, S., Reynolds, J., Nielsen, L. L., Parkes, D. G., and Young, A. A. (2005) Dose-response for glycaemic and metabolic changes 28

days after single injection of long-acting release exenatide in diabetic fatty Zucker rats, *Diabetologia 48*, 1380-1385.

46. Vrang, N., Jelsing, J., Simonsen, L., Jensen, A. E., Thorup, I., Soeborg, H., and Knudsen, L. B. (2012) The effects of 13 wk of liraglutide treatment on endocrine and exocrine pancreas in male and female ZDF rats: a quantitative and qualitative analysis revealing no evidence of drug-induced pancreatitis, *Am. J. Physiol. Endocrinol. Metabol. 303*, E253-264.

47. Jelsing, J., Vrang, N., Hansen, G., Raun, K., Tang-Christensen, M., and Knudsen, L. B. (2012) Liraglutide: short-lived effect on gastric emptying -- long lasting effects on body weight, *Diabetes Obes. Metab. 14*, 531-538.

48. Santi, D. V., Schneider, E. L., and Ashley, G. W. (2014) Macromolecular prodrug that provides the irinotecan (CPT-11) active-metabolite SN-38 with ultralong half-life, low C(max), and low glucuronide formation, *J. Med. Chem. 57*, 2303-2314.

49. Fehse, F., Trautmann, M., Holst, J. J., Halseth, A. E., Nanayakkara, N., Nielsen, L. L., Fineman, M. S., Kim, D. D., and Nauck, M. A. (2005) Exenatide augments first- and second-phase insulin secretion in response to intravenous glucose in subjects with type 2 diabetes, *J. Clin. Endocrinol. Metab. 90*, 5991-5997.

50. Drucker, D. J., Buse, J. B., Taylor, K., Kendall, D. M., Trautmann, M., Zhuang, D., and Porter, L. (2008) Exenatide once weekly versus twice daily for the treatment of type 2 diabetes: a randomised, open-label, non-inferiority study, *Lancet 372*, 1240-1250.

51. Kim, D., MacConell, L., Zhuang, D., Kothare, P. A., Trautmann, M., Fineman, M., and Taylor, K. (2007) Effects of once-weekly dosing of a long-acting release formulation of exenatide on glucose control and body weight in subjects with type 2 diabetes, *Diabetes Care 30*, 1487-1493.

52. O'Connor-Semmes, R. L., Lin, J., Hodge, R. J., Andrews, S., Chism, J., Choudhury, A., and Nunez, D. J. (2014) GSK2374697, a novel albumin-binding domain antibody (AlbudAb), extends systemic exposure of exendin-4: first study in humans--PK/PD and safety, *Clin. Pharmacol. Ther. 96*, 704-712.

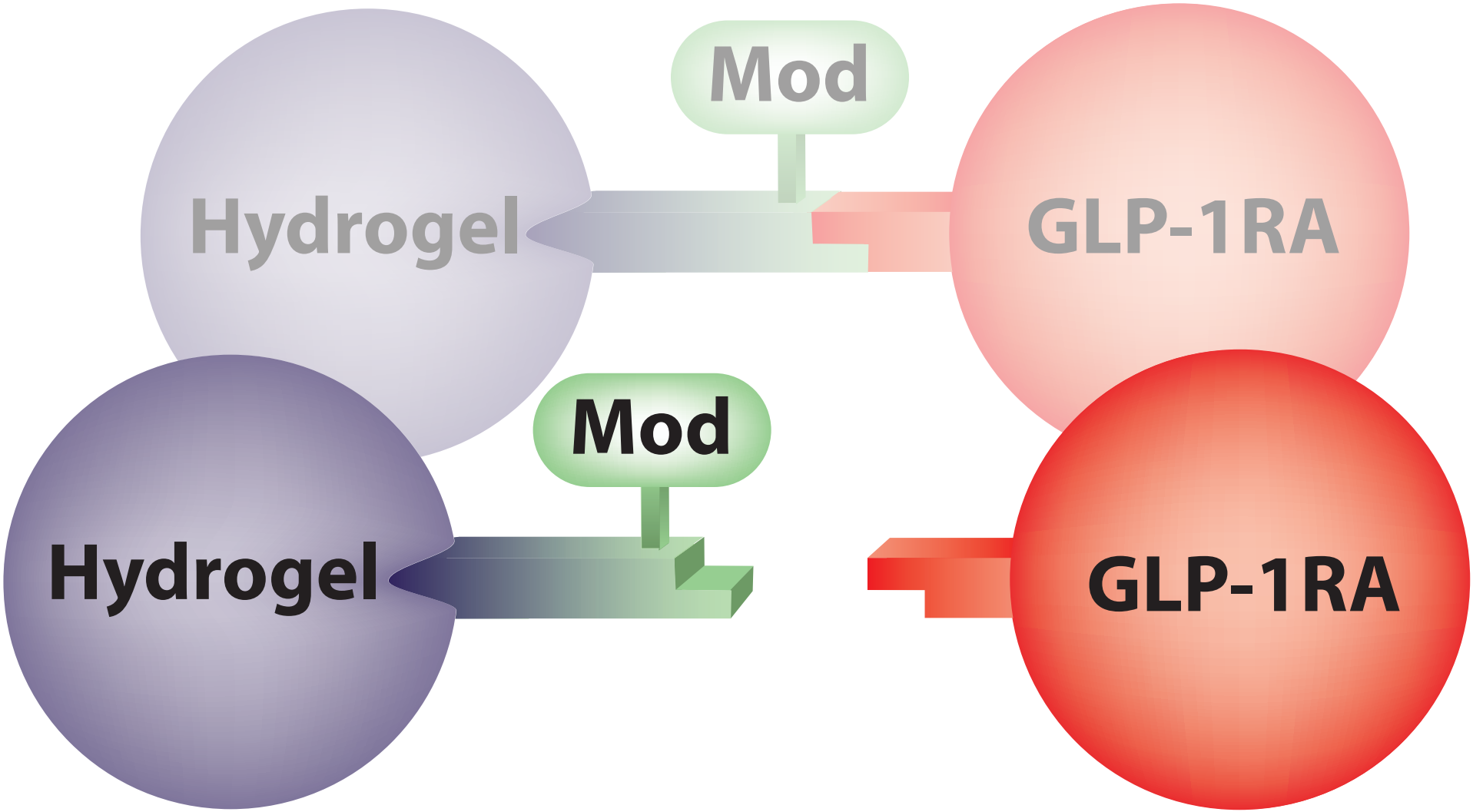
Mod
Hydrogel
GLP-1RA
Mod
Hydrogel
GLP-1RA